Surface Impedance Imaging Technique

ARTICLE *in* ANALYTICAL CHEMISTRY · AUGUST 2008

Impact Factor: 5.64 · DOI: 10.1021/ac800361p · Source: PubMed

3 AUTHORS:

Kyle J Foley
Arizona State University
9 PUBLICATIONS **228** CITATIONS
SEE PROFILE

Xiaonan Shan
Arizona State University
36 PUBLICATIONS **473** CITATIONS
SEE PROFILE

Nongjian Tao
Arizona State University
223 PUBLICATIONS **12,956** CITATIONS
SEE PROFILE

Article

Surface Impedance Imaging Technique

Kyle J. Foley, Xiaonan Shan, and N. J. Tao

Anal. Chem., **2008**, 80 (13), 5146-5151• DOI: 10.1021/ac800361p • Publication Date (Web): 17 May 2008

Anal. Chem. **2008,** *80,* 5146–5151

Surface Impedance Imaging Technique

Kyle J. Foley, Xiaonan Shan, and N. J. Tao*

Department of Electrical Engineering, Arizona State University, Tempe, Arizona 85287

We demonstrate here a surface impedance imaging technique based on sensitive dependence of surface plasmon resonance (SPR) on local surface charge density. By applying a potential modulation to a sensor surface, we are able to simultaneously obtain three images: the dc component and the amplitude and phase of the ac component. The dc image measures local molecular binding activity on the surface, as found in the conventional SPR imaging technique, and the ac images are directly related to the local impedance of the surface. Our experimental data can be analyzed quantitatively in terms of the simple free electron gas model for the sensor surface and the Randles equivalent circuit model for interfacial impedance.

Interfacial impedance spectroscopy has been widely used as a powerful technique to study various surface and electrochemical processes as well as a sensitive signal transduction method for chemical and biosensors.[1] To date, interfacial impedance spectroscopy has been performed on a single electrode or an array of electrodes in which each electrode is individually connected to a measurement circuit. For many applications, ranging from surface corrosion to protein and DNA microarrays, it is highly desired to image or map the local impedance of the entire electrode and sensor surfaces, which so far has not been demonstrated. Here we present a method that can image local interfacial impedance. Since the method is based on surface plasmon resonance (SPR) detection, it also allows simultaneous conventional SPR imaging to provide additional information on local molecular binding and interfacial processes.

The basic principle of our technique is that SPR is sensitive to the surface charge density of the electrode or sensor, which has been studied using electroreflectance spectroscopy.[2,3] In a typical SPR imaging setup, a p-polarized collimated beam from a laser or a light-emitting diode (LED) is incident upon a thin metal film (sensor or electrode) through a prism, and light reflected from the metal film is detected by an imaging device (Figure 1A). At an appropriate incident angle (called resonance angle), light excites collective oscillations of conduction electrons in the metal film, known as surface plasmons, which causes a sharp decrease in the reflection of light. Since the resonance angle is sensitive to molecular binding taking place on or near the metal film, SPR has emerged as a label-free detection method in biosensors. In contrast, impedance spectroscopy is based on an entirely different principle. Interfacial differential impedance is defined by $Z = \Delta V/\Delta I$, where ΔV is a potential modulation applied to an electrode and ΔI is the current response to the potential modulation. Since ΔI usually has a different phase from ΔV, Z is described by a complex number (or amplitude and phase). Z is very sensitive to the properties of the electrode surface and to molecular adsorption taking place on the electrode surface, which is the basis of impedance spectroscopy for studying interfacial phenomena and biosensor applications.

By measuring SPR in an electrolyte, we can obtain interfacial impedance by applying a potential modulation to the sensor surface. This is because the potential modulation causes a surface charge modulation which changes the surface plasmons in the metal film. By measuring the amplitude and phase of the resonance angle, we can obtain interfacial impedance information. We have demonstrated before that a modulation in the resonance angle smaller than 10^{-6} deg can be measured,[4] so accurate imaging of surface impedance is possible based on SPR detection.

A quantitative relation between SPR angle modulation and interfacial impedance can be derived based on the following analysis. First, the resonance angle, θ_R, depends on the dielectric constant of the metal film, ϵ_m, according to[5]

$$\sin(\theta_R) = \sqrt{\frac{\varepsilon_1 \varepsilon_m}{(\varepsilon_1 + \varepsilon_m)\varepsilon_2}} \tag{1}$$

where ϵ_1 and ϵ_2 are the dielectric constants of the buffer solution and prism, respectively. ϵ_m depends on the surface charge density, which is the reason that the SPR resonance angle is sensitive to the surface charge density. An explicit relationship between ϵ_m and surface charge density can be obtained based on the Drude model, a free electron gas model for metals.[6] According to the Drude model, ϵ_m of the metal film as a function of frequency, f, is given by

$$\varepsilon_m(f) = 1 - \frac{n_e e^2}{\varepsilon_0 m_e 4\pi^2 f^2} \tag{2}$$

where e, m_e, and n_e are the electron charge, mass, and density, respectively, and $\epsilon_0 = 8.85 \times 10^{-12}$ F/m. For a thin metal film of

* Corresponding author. E-mail: njtao@asu.edu.

(1) Katz, E.; Willner, I. *Electroanalysis* **2003**, *15*, 913–947.
(2) McIntyre, J. D. *Surf. Sci.* **1973**, *37*, 658–682.
(3) Kotz, R.; Kolb, D. M.; Sass, J. K. *Surf. Sci.* **1977**, *69*, 359–364.
(4) Wang, S.; Boussaad, S.; Wong, S.; Tao, N. J. *Anal. Chem.* **2000**, *72*, 4003–4008.
(5) Orlowski, R.; Raether, H. *Surf. Sci.* **1976**, *54*, 303–308.
(6) Kittel, C. *Introduction to Solid State Physics*, 8th ed.; John Wiley & Sons: New York, 2005.

10.1021/ac800361p CCC: $40.75
Published on Web 05/17/2008

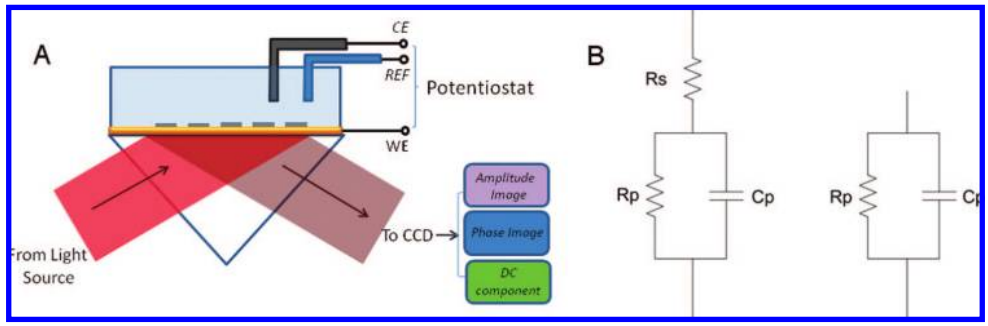

Figure 1. (A) Schematic of experimental setup and (B) equivalent circuits used in modeling surface impedance showing the Randles equivalent circuit (left) and the two-component model with parallel resistor and capacitor (right).

thickness d_m, a change in the surface charge, $\Delta\sigma$, gives rise to a change in the electron density according to

$$\Delta\sigma = -ed_m\Delta n_e \tag{3}$$

Substituting eq 2 into eq 3, we express the charge density change in terms of the metal dielectric constant change

$$\Delta\sigma = -\frac{ed_m n_e}{\varepsilon_m - 1}\Delta\varepsilon_m \tag{3'}$$

Combining eqs 1 and 3′, we find that the relationship between the surface charge change ($\Delta\sigma$) the resonance angle shift ($\Delta\theta_R$) is given by

$$\Delta\sigma = \alpha\Delta\theta_R \tag{4}$$

where

$$\alpha = -\frac{ed_m n_e \varepsilon_2(\varepsilon_1 + \varepsilon_m)^2 \sin(2\theta_R)}{\varepsilon_1^2(\varepsilon_m - 1)} \tag{5}$$

In the present experiment, $\epsilon_1 = 1.77$ (water), $\epsilon_2 = 2.29$ (BK7 prism), $d_m = 47$ nm, $n_e = 5.9 \times 10^{-28}$ m^{-3}, and $\epsilon_m = -11.7$ for the Au film, $\theta_R = 72°$ according to eq 1. The calculated α based on eq 5 is $\alpha_{cal} = 28$ C m^{-2} deg^{-1}.

Finally, since surface charge density is related to interfacial capacitance density (capacitance per unit area), c, by

$$\Delta\sigma = c\Delta V \tag{6}$$

where ΔV is the potential change, which can be modulated and controlled using a standard electrochemical setup, one can image the interfacial capacitance by monitoring the local SPR response due to the applied potential modulation by

$$c(x,y) = \alpha\Delta\theta_R(x,y)/\Delta V \tag{7}$$

The above analysis establishes a simple relation between local interfacial capacitance and local potential-modulated SPR angle, which is the basic principle of our interfacial impedance imaging technique. As we will see later, the Drude model provides a semiquantitative description of our experimental data. When the Drude free electron gas model is replaced by a more sophisticated theory, we expect the above conclusion still holds except that α will be replaced by a more accurate number.

One assumption made in deriving the above relation is that the resistance of the electrolyte or buffer solution is negligible. Although this assumption is reasonable in many cases, a more complete model (e.g., Randles equivalent circuit model[7]) treats the metal−solution interface by a capacitor, C_p, in parallel with a resistor, R_p, and the solution phase resistance by a resistor, R_s (Figure 1B). As we will discuss later, this extra resistance introduces a phase shift between the resonance angle modulation, $\Delta\theta_R(x, y)$, and the potential modulation, ΔV. In this case, we can obtain both amplitude and phase images of the surface.

EXPERIMENTAL SECTION

The SPR imaging setup is based on the widely used Kretschmann configuration (Figure 1A).[8] The optical system is comprised of an LED light source (670 nm), collimating lens, prism, imaging optics, polarizer, and a charge-coupled device (CCD) camera. Initially the collimated incident beam was adjusted and then fixed at an angle where the reflectivity detected by the CCD was ~50% of the maximum intensity. A local shift in the resonance angle causes a change in the measured reflectivity which was imaged with the CCD. The SPR image was captured at up to 380 frames/s, allowing for measurements of the SPR response induced by the applied potential modulation. The images were recorded at a bit depth of 14 bits with a maximum resolution of 320 × 240 pixels. An image captured signal (square wave) was recorded from the camera to allow for synchronizing the image with the electrochemical current and potential data measured in concert. An electrochemical cell was made of Teflon using a silver wire as quasi reference electrode and a platinum wire as counter electrode. The potential of the sensor surface was controlled using a bipotentiostat (Pine ARFDE5), and a sinusoidal potential modulation was applied with a function generator (Hewlett-Packard 33120A). The modulation frequency ranged from 1 to 70 Hz at an amplitude up to 100 mVpp. Typically, a total of 10 000 images were capture along with modulating potential and electrochemical current. The data collection was achieved using a PC with LabView software for voltage and current acquisition and image capturing software via FireWire 800 (IEEE 1394b). Post-processing of data was accomplished using a program written in MATLAB.

(7) Bard, A. J.; Faulkner, L. R. *Electrochemical Methods*, 2nd ed.; Wiley: New York, 2001.
(8) Kretschmann, E. *Z. Phys.* **1971**, *241*, 313–324.

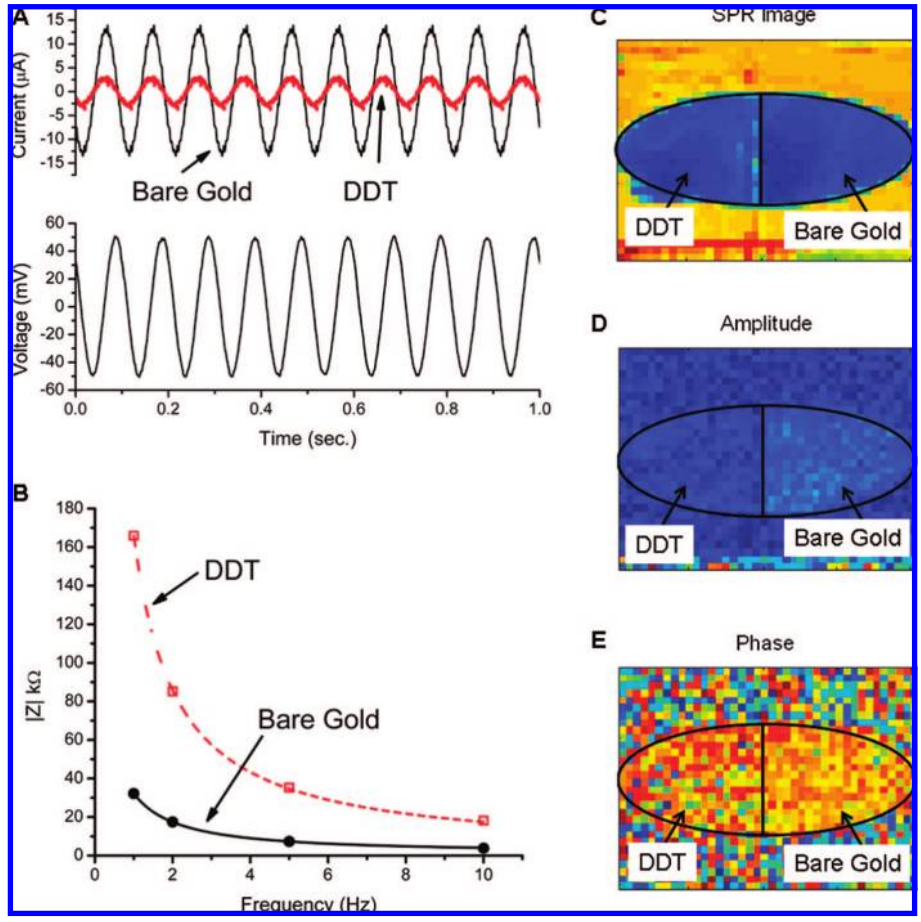

Figure 2. Results from the two divided area experiments. (A) Electrochemical current modulations of the bare (larger amplitude, thin line) and DDT-covered (smaller amplitude, thick line) areas as a result of a 10 Hz modulating potential. (B) Measured (dots) and fit (lines) impedance amplitudes vs frequency for the bare (solid line) and DDT-covered (dashed line) areas. (C) Direct current component image of the SPR response showing contrast due to molecular adsorption. The elliptical region is the region exposed to solution that is divided into two areas near the center, and the area outside the ellipse is outside of the solution cell. (D) Amplitude image of the SPR modulation. (E) Phase image of the SPR modulation.

The sensor chip was a BK7 glass coverslip coated with ~2 nm of chromium followed by ~47 nm of gold. Each chip was briefly annealed with a hydrogen flame to remove surface contamination. To demonstrate the impedance imaging capability, an array of 1-dodecanethiol (DDT) spots was created on the sensor surface using the PDMS contact printing method.[9] The PDMS stamp was first submerged in a ~10 mM thiol solution for ~5 min and placed onto the gold surface after drying with nitrogen gas. Then after a minute the stamp was removed, and the gold slide with the thiol pattern was placed upon the prism with refractive index matching oil between them. The electrochemical SPR cell was mounted on the sensor chip, and 50 mM Tris buffer (pH = 8) was introduced into the cell.

RESULTS AND DISCUSSION

We carried out the initial test of the principle using a gold film that is divided into two electrically isolated areas. The electrical isolation is needed for measuring the impedance of the two areas independently using the standard impedance analysis. The two areas were exposed to the same electrolyte and shared the same reference and counter electrodes, and the working electrode potentials are controlled with the bipotentiostat. The currents through the two working electrodes were monitored independently. In order to observe the relative contrast of the two areas, we coated one area with DDT using a PDMS stamp and left the other bare. By applying an ac modulation to the potentials of the two areas, we were able to measure the impedance of the two areas and image the SPR responses simultaneously.

We measured the impedance of the two areas by recording the amplitude of the current modulation and the phase shift of the current modulation relative to the applied potential of at various frequencies and amplitudes of the potential modulation (Figure 2, parts A and B). The results were fitted using the Randles model (Figure 1B). The fitting parameters were R_p = 74 ± 20 kΩ and C_p = 4.6 ± 0.3 μF for the bare gold side and R_p = 570 ± 60 kΩ and C_p = 0.92 ± 0.01 μF for the DDT side. The interfacial resistance, R_p, for the DDT-covered surface is much greater than that for the bare gold electrode, which is expected considering the blockade of interfacial charge transfer by the DDT layer. The interfacial capacitance, C_p, of the DDT surface is much smaller than that of the bare gold electrode, which is also expected due to the difference in the adsorbed layer's dielectric constant and the increased double layer thickness of the DDT-covered electrode. The corresponding

(9) Kumar, A.; Biebuyck, H. A.; Whitesides, G. M. *Langmuir* **1994**, *10*, 1498–1511.

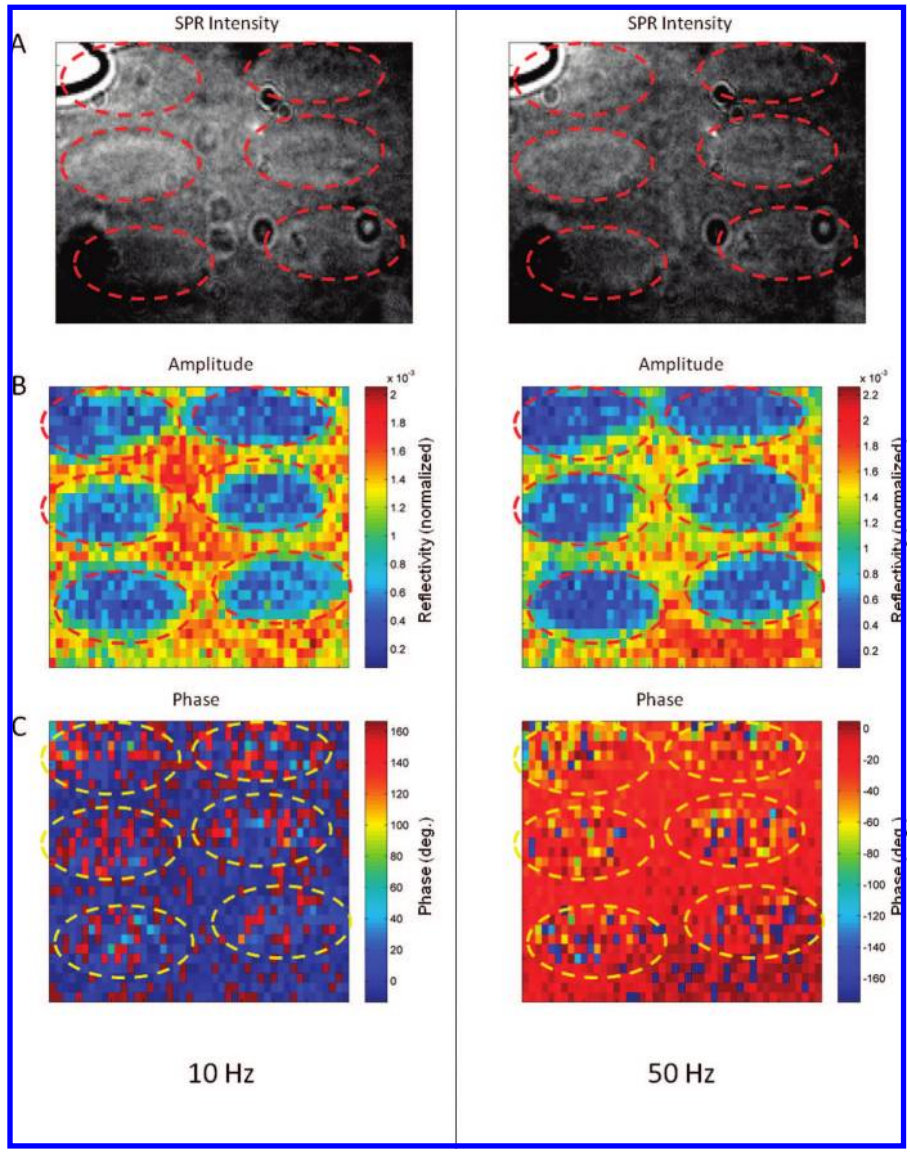

Figure 3. (A) SPR image, (B) amplitude, and (C) phase images at 10 and 50 Hz. The spots were created using a PDMS stamp soaked in ~10 mM DDT solution and then placed on the gold surface for 30 s. The elliptical areas show the printed DDT regions. The contrast of the image has been changed to enhance the image.

capacitance per unit area for the bare gold is ~47 μF/cm^2, which is in good agreement with literature.[10] The capacitance per unit area for the DDT-coated surface is 9.4 μF/cm^2, which is higher than reported in literature.[11] We believe that this difference is due to low coverage and imperfect packing of DDT layer formed by the contact printing approach in our experiment. This observation is supported by the SPR data which will be discussed next. The solution resistance, R_s = ~2 kΩ, is much smaller than the interfacial charge transfer resistance. So to a first-order approximation, we may assume a negligible solution resistance.

Our SPR measures reflectivity change due to the shift in the resonance angle. Within an angular range of ~1.5°, the resonance angle shift is linearly proportional to the reflectivity change, and the calibration coefficient was determined by performing numerical simulation and experimental calibration. The simulation using Winspall, an SPR modeling program,[12] gives a coefficient of 0.045° per 1% reflectivity change. The experimental calibration measured reflectivity change for a given shift in the incident angle, which led to a similar coefficient of 0.044° per 1%. The SPR response includes a dc component in the resonance angle that provides the coverage and thickness information of molecules adsorbed on the sensor surface. It contains also an ac modulation in the resonance angle resulted from the applied potential modulation (Figure 2C−E). Figure 2C shows the dc component image. The reflectivities of the two areas were determined from the SPR image, and they were 54.74% and 58.47%, respectively. From the contrast difference and the calibration coefficient, we determined that the DDT area has an average resonance angle of ~10 mdeg greater than that of the bare gold area. The difference in the resonance angles between the bare and the DDT areas corresponds to a thickness of ~1 nm if the dielectric constant of 2.10

(10) Hamelin, A.; Vitanov, T.; Sevastyanov, E.; Popov, A. *J. Electroanal. Chem.* **1983**, *145*, 225–264.
(11) Porter, M. D.; Bright, T. B.; Allara, D. L.; Chidsey, C. E. D. *J. Am. Chem. Soc.* **1987**, *109*, 3559–3568.
(12) Worm, J.; Knoll, W. http://www.mpip-mainz.mpg.de/knoll/soft/.

for the DDT film is assumed.[13] This value is smaller than the thickness of a perfectly ordered DDT monolayer (~1.4 nm),[14] indicating an imperfect coverage of DDT as found also from the impedance measurement discussed above.

The ac component of the SPR response includes both the amplitude and phase information. The local amplitude and phase information of the sensor surface was extracted by performing a fast Fourier transform (FFT) on each pixel of the CCD imager, which created an amplitude image and a phase image (Figure 2, parts D and E). To improve the signal-to-noise ratios of the amplitude and phase images, a group of pixels can be selected, and the averaged amplitude and phase information was determined to create images. This approach does sacrifice the spatial resolution, so one must optimize the spatial resolution and signal-to-noise merit according to the needs of different applications. The amplitude image shows that the resonance angle modulation induced by a 0.05 V modulation in the potential is $\sim 3 \times 10^{-4}$ deg, or ~9 mdeg/V, for the bare gold area. This value is only slightly smaller than ~10 mdeg/V reported in literature.[15] Using the measured ~9 mdeg/V modulation and interfacial capacitance of 47 μF/cm^2, we found that $\alpha_{exp} = 47$ C m^{-2} deg^{-1}, which is in excellent agreement with $\alpha_{cal} = 28$ C m^{-2} deg^{-1} calculated using the crude free electron gas model.

The average modulation amplitude in the resonance angle for the DDT area is 1.3×10^{-4} deg, smaller than that of the bare gold electrode. Using α_{exp}, we find the interfacial capacitance is ~12 μF/cm^2, which is somewhat greater than the directly measured capacitance value. Given the error bar in α_{exp} and the neglect of the finite resistance of the solution phase, this agreement is considered to be good. Without solution resistance, the modulation in the resonance angle should be always in phase with the applied potential modulation, and the phase image should show little contrast. As shown in Figure 2E, the contrast of the phase image is indeed small, but not zero. The nonzero phase contrast is due to the small but finite solution phase resistance. As we will discuss later, the phase shift in the resonance angle increases with the modulation frequency, which can be fully described by including a finite solution phase resistance in the Randles model.

The experiments described above demonstrate a simultaneous SPR and interfacial impedance imaging capability and also confirm the principle of the technique. Local interfacial impedance information may be possible by the conventional surface impedance analysis techniques using an array of individually addressed electrodes. However, a large electrode array demands sophisticated microfabrication, and simultaneous impedance measurement of all the electrodes requires massive electrical connection and complicated impedance analysis circuits. Furthermore, the use of an array of electrically isolated electrodes creates a heterogonous surface that is not suitable for many DNA and protein microarray technologies. The most attractive feature of the present method is that the local impedance can be mapped out with micrometer-level resolution without the need of dividing the sensor surface into electrically insulated electrodes. To demonstrate the unique feature, we printed an array of DDT onto a gold sensor surface using the microcontact printing approach described in the Experimental Section. Different from the first set of experiments where the sensor surface is divided into two electrically isolated areas, here the individual elements of the array are printed on the same electrode surface. So the conventional impedance analysis cannot be used to obtain the impedance of each element.

Figure 3A shows the dc component image of the surface which resolves a 3×2 array of DDT similar to the conventional SPR imaging technique. The areas marked by circles are covered with DDT, and outside of the circles is bare gold surface. The amplitude and phase images are shown in Figure 3, parts B and C, at two different modulation frequencies. The amplitude image shows a better contrast than the conventional SPR imaging mode (dc component), indicating a potentially more sensitive detection of molecular binding on surfaces. The negative contrast of the amplitude image is due to that the DDT-covered areas have smaller capacitance than the bare gold surface. The phase image shows a very small contrast of the array indicating a relatively small phase difference between the DDT-covered and bare gold surfaces. As we have already discussed, in the absence of solution phase resistance, the phase image should have zero contrast and both the amplitude and phase images should not be dependent on the modulation frequency. However, a small phase contrast is observed and the amplitude contrast depends on the modulation frequency, which indicates the importance of the solution phase resistance. Using the Randles model, we found that for a given applied modulation, ΔV_{app}, the actual potential modulation across the metal−solution interface is given by

$$\Delta V_{\text{interface}} = \frac{R_p}{R_p + R_s + j2\pi f R_p R_s C_p} \Delta V_{app} \qquad (8)$$

where C_p is the total capacitance of the metal−solution interface and is location-dependent (see eq 7). The local resonance angle is obtained by replacing ΔV_{app} in eq 7 with eq 8 and substituting in $C_p(x, y)$ in the place of $c(x, y)$ with the dependence on spatial location shown, which then takes the form of

$$\Delta\theta_R(x,y) = \frac{R_p C_p(x,y)}{\alpha(R_p + R_s + j2\pi f R_p R_s C_p(x,y))} \Delta V_{app} \qquad (9)$$

To verify the analysis, we have determined the modulation amplitude and phase shift for both the bare gold surface and DDT elements (Figure 4). Both the amplitude and phase decrease with frequency, as predicted by the simple model. The frequency-dependent amplitude and phase can be fit with eq 9 using nonlinear least-squares methods with fitting parameter $\beta = (2\pi CRR_s/(R + R_s))^2 = 4.5 \times 10^{-4}$ for the bare gold area and 2.4×10^{-4} for the DDT area. Using the low-frequency amplitude values for the bare and DDT regions, we found that the interfacial capacitance values were equal to 50.7 and 12.7 μF/cm^2, respectively. These correspond well with the values measured in the two area experiment described earlier.

The analysis shows that just like conventional impedance spectroscopy one can obtain important interfacial parameters in terms of model resistors and capacitors by performing the

(13) Peterlinz, K. A.; Georgiadis, R. *Langmuir* **1996**, *12*, 4731–4740.
(14) Barrena, E.; Ocal, C.; Salmeron, M. *J. Chem. Phys.* **2000**, *113*, 2413–2418.
(15) Tao, N. J.; Boussaad, S.; Huang, W. L.; Arechabaleta, R. A.; D'Agnese, J. *Rev. Sci. Instrum.* **1999**, *70*, 4656–4660.

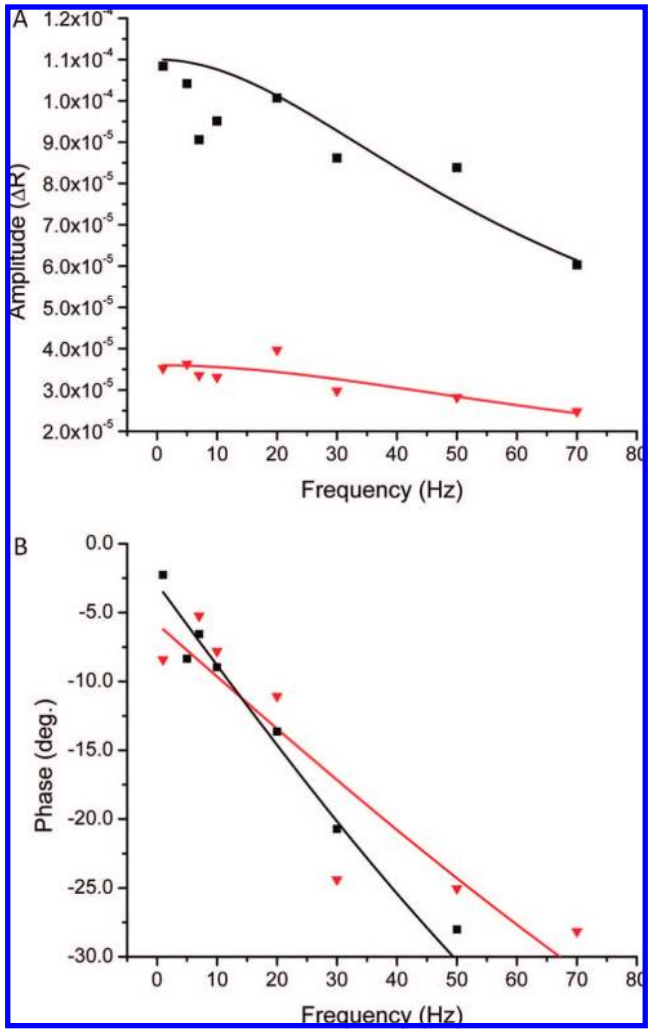

Figure 4. (A) Amplitude and (B) phase comparison of a DDT array element (T) and a bare gold element (S). The amplitude of the DDT element is smaller than that of the bare gold element. Extracting the capacitance values from the curve fits for the amplitude resulted in values of 50.7 μF/cm^2 for the bare gold and 12.7 μF/cm^2 for the DDT spot.

measurement as a function of modulation frequency. The highest possible frequency is limited by the imaging device which is less than 1 kHz in the present case. However, CCDs with extremely fast frame rates (~1 million frames/s) are already commercially available which could expand the upper limit to approximately megahertz. Furthermore, the rapid development of CMOS imaging sensors will lead to faster and cheaper imaging devices.

CONCLUSION

We have demonstrated a technique to image surface impedance in solution, which expands the powerful surface impedance analysis from spectroscopy to microscopy and local spectroscopy. The basic principle relies on the sensitive dependence of the SPR angle on surface charge density which can be modulated by applying an ac modulation to the potential of the sensor surface. The dc component of the SPR signal is the same as the conventional SPR image, which provides molecular binding information. In contrast, the ac component is the SPR response to the surface charge modulation. Using FFT we have extracted the local amplitude and phase of the ac component and obtained both the amplitude and phase images at various frequencies. The measured SPR angle modulations agree with the simple free electron gas model for the metal film (SPR sensor surface), and the frequency dependence of the amplitude and phase images are well described by the Randles equivalent circuit model. The interfacial capacitance values obtained from the amplitude and phase images are in good agreement with the values measured using the conventional impedance analysis method. In addition to providing local impedance information of the sensor surface, the ac images may help us to reveal features not possible with the conventional SPR imaging techniques. We believe that the technique will be useful for studying fundamental phenomena taking place on an electrode surface and for biosensor and biochip applications.

ACKNOWLEDGMENT

This work was supported in part by the NIH under Grant NIH 1 U01 ES016064-01.

Received for review February 20, 2008. Accepted April 12, 2008.

AC800361P